Evaluation of joint type modelling in the human hand

Agneta Gustus[c,d], Patrick van der Smagt[a,b,d]

[a]*Technische Universität München, Arcisstraße 21, 80333 München, Germany.*
[b]*fortiss, Guerickestraße 25, 80805 München, Germany.*
[c]*Klinikum rechts der Isar der TU München, Ismaninger Straße 22, 81675 München, Germany.*
[d]*www.brml.org*

Abstract

This short communication presents preliminary results from an extensive investigation of joint modelling for the human hand. We use finger and hand movement data recorded from both hands of 110 subjects using passive reflective markers on the skin. Furthermore, we use data which was recorded from a single Thiel-fixated cadaver hand using also passive reflective markers but fixed to the bone. Our data clearly demonstrate that, for wrist and finger joints, hinge joint models are sufficiently accurate to describe their movement in Cartesian space.

Keywords: human hand model, joint model, wrist, metacarpophalangeal joint (MCP), proximal interphalangeal joint (PIP), distal interphalangeal joint (DIP)

1. Introduction

For understanding human hand functionality proper joint modelling is crucial. The range of available simulations spread from hinge joints (1; 2; 3; 4) over double hinge joints (called ovoid motion in (5), obtained by geometric measurements) to costly multibody simulations (6; 7) and combined multibody finite-element simulations (8).

We present an objective measure for deciding which joint model type should be used for a simulation by providing a numerical measurement on goodness of fit. For this purpose we use the sample deviation between the recorded marker position and the modelled marker position and the ANOVA F-test to verify the difference of both joint model approaches, viz. hinge joint and double hinge joint. Therefore we investigated joint movements of the middle finger using a Thiel-fixated human left hand specimen, by fixing motion tracking markers directly to the bone, and compared the results with movements recorded from human hands where the markers are either glued to the skin or clamped to the finger of healthy volunteers.

2. Methods

We obtained two data sets of movement measurements data from human hands. The first data set is from a cadaver hand provided by the *Anatomische Anstalt* of the *Ludwig Maximilians* University in Munich. This specimen is a Thiel-fixated left hand, of a 78-year old woman, dissected at half-length of the radius and ulna. The tendons were carefully prepared proximal to the carpal tunnel and sewed using a Krakow suture to 0.6 mm Dyneema threads. In the bones of the middle finger screws with 1.5 mm diameter were carefully placed not disturbing joint functionality and tendon function. Marker trees, each with four marker spheres of diameter 4 mm, were glued onto the screw heads Fig. 1 (a). The movement was initiated by pulling either the corresponding flexor or extensor tendons using a weight-based testbed leading in a flexion extension movement of wrist, metacarpophalangeal (MCP), proximal interphalangeal (PIP) and distal interphalangeal (DIP) joint of the middle finger recorded at 100 Hz with an 8-camera VICON MX3+ passive motion tracking system.

The second data set, called "219 hands", was recorded at the German Aerospace Center (DLR) where it was obtained by recording movement of both hands of 110 volunteers, 67 male and 43 female, age between 9 and 65 years. Since one person wore a splint on one arm, we only recorded 219 hands in total. Movement was recorded with a 6-camera VICON T20 tracking system at 100 Hz using passive marker trees, as described above, attached on proximal and distal phalanges by clips which wrapped around three quarter of the finger and were glued onto skin of the dorsal side of the hand. For middle phalanges we glued single half spheres reflective markers on the skin in the middle of the phalanges Fig. 1 (d). This arrangement was due to the limited numbers of cameras available and the optimisation of visibility of all markers in the camera setup. It has a drawback of skin-induced marker movement, leading to systematic errors in the data (9). Whereas the clips with the marker trees are supposed to suppressed this behaviour by tightly clamping around the side of the fingers. Further examining of the induced error we explain in Sec. 4. Subjects were asked to follow a strict movement protocol in which full movement ranges of all marked fingers were recorded: 1. flat hand, 2. DIP 2-5 flexion/extension, 3. DIP and PIP 2-5 flexion/extension, 4. spread all fingers, 5. finger 2 adduction/abduction, 6. finger 2 circumduction, 7. finger 3 adduction/abduction, 8. finger 3 circumduction, 9. finger 4 adduction/abduction, 10. finger 4 circumduction, 11. finger 5 adduction/abduction, 12. finger 5 circumduction, 13. finger 1 adduction/abduction, 14. IP flexion/extension, 15. IP and MCP1 flexion/extension, 16. finger 1 circumduction, 17. fingers 1 and 5 opposition, 18. MCP 2-5 flexion/extension, 19. wrist flexion/extension, 20. wrist adduction/abduction, and 21. wrist circumduction.

From both data sets the markers were labelled using the VICON Nexus software, and subsequently exported to Matlab. In Matlab the data sets were cleaned from outliers caused by erroneous automatic labelling.

After that each segment of the finger was assigned a fixed coordinate systems (CS), e.g., we denote the coordinate system of a proximal phalanx by

CSPP. Then the marker or markers of the next more distal finger segment were transformed into the next proximal CS by applying a homogeneous coordinate transformation; e.g., the marker(s) of the middle phalanx (MP) were transformed into the CSPP. Meaning that CSPP was now a steady base $(0,0,0)$ with identity rotation matrix and we obtained the the pure movement of the MP markers in the coordinate system of CSPP.

The resulting data points were gathered in a matrix $\mathbf{A}$ of dimensions $N \times 3$, with N the number of recorded frames. Using PCA and keeping only the first two principal components, this matrix was linearly transformed to a matrix $\mathbf{A}'_2 = \mathbf{A}\mathbf{B}_2$ with $\mathbf{B}_2$ a 3×2 matrix. The resulting matrix $\mathbf{A}'_2$ has dimensions $A \times 2$, putting the data in a coordinate frame where maximal variance—and thus maximal movement—is situated amongst its axes. For all joints the flexion/extension movement data was linearly mapped to 2D by selecting the two principal components after PCA.

The resulting data was subsequently fitted to a circle using the method described in (10), an algebraic fit which centres the data and uses its normed matrix of moments for polynomial optimisation using the Newton–Raphson method; 20 iterations suffice. After that the circle centre and radius are calculated. To compare the fit to the double ovoid joint model postulated in (5), we also fitted the data to two circles for comparison as ovoid motion could be described by stringing together different ring segment motion. Hence, the data was divided in two subsets, named dorsal and volar, to fit circles to each subset using the method from (10). To find these subsets, the data (N samples) was evenly split in 100 joint angle segments Θ_{cut}, and for each split a hinge joint was fitted using the same method as described before resulting in two radii r_{dorsal} and r_{volar}. For each fit, dorsal and volar, the sample standard deviation was calculated to quantify the overall sample standard deviation s taking the number of samples, dorsal (B) and volar ($N - B$), into account. We compute the overall standard deviation for every possible split and select the smallest, using

$$s = \min\left(\Theta_{\mathrm{cut}}, \sqrt{\frac{1}{B-1}\sum_{i=1}^{B}(r_i - r_{\mathrm{dorsal}})^2}\,\frac{B}{N} + \sqrt{\frac{1}{N-B-1}\sum_{i=B+1}^{N}(r_i - r_{\mathrm{volar}})^2}\,\frac{N-B}{N}\right)$$

Additionally we apply an ANOVA F-test to the radii to assess if the two fits differ significantly. Following F-test statistics, as we have two types of data modelling the "between-group degrees of freedom" f_b is 1 and the "within-group degrees of freedom" f_w is $2 \cdot N - 1$, as the samples per group is higher than 1000 we have a critical $\mathrm{F}(f_b = 1, f_w = \infty)$ value of 6.635 using an α of 0.01, meaning a 1% significance level. We apply the same calculations for the PIP, DIP, MCP and wrist joints of the 219 hands data set.

3. Results

The joint fits are demonstrated on the left hand specimen in Figures 1b–1c and on right hand of Subject 1 in 1e–1i. The data is plotted in the movement plane of flexion/extension for each joint.

3

Table 1: Sample standard deviation s for the different joint models hinge joint (hj) and double hinge joint (double hj) for the cadaver hand; tolerable centre of rotation (CoR) for double hinge joint; F-test values where F critical is 6.635 (11) for alpha 0.01

Joint	Movement range (deg)	s		F- test value
		hj	double hj	
specimen				
PIP	64	0.25	0.21	$4 \cdot 10^{-3}$
wrist	120	0.70	0.45	10^{-5}
subject 1				
PIP finger 2	94	0.35	0.30	1.15
MCP finger 2	64	0.31	0.30	$2 \cdot 10^{-6}$
MCP finger 3	96	0.28	0.21	10^{-3}
DIP finger 3	91	0.34	0.32	0.25
wrist	141	1.92	1.70	0.03

As mentioned in Sec. 2, the nonrigid marker attachment for the 219 hands data set induces aberrant marker movement in DIP and PIP (exemplarily marked in Fig. 1 (h)). The skin movement is expected to influence our modelling, and we expect lower accuracies than for the Thiel-fixated specimen, in which the markers are directly connected to the bones.

After evaluating the standard deviation and F-test value in DIP, PIP, or MCP joints of the human hand 1, we found no evidence of double hinge joint motion as postulated in (5). The data from the Thiel-fixated hand is fitted very well by a circle (sample standard deviation between 0.2–0.3 mm and F-test value below 0.01 for the circle radii). Evaluating the subject data we conclude single circle fits are sufficient (sample standard deviation around 0.4 mm, F-test value below 1.6 for the circle radii).

Looking at the numerically optimised CoRs of the double-hinge joint fit, we find the fits found through numerical optimisation are radically different from those postulated in (5). In our data, the "ovoid shift" is more than 1.5 cm and the radii differ significantly, with CoRs often lying far outside the finger. The sample standard deviation of the double hinge joint fit is better than the hinge joint fit, but only at less than 1% significance.

We performed the same analyses for wrist flexion/extension, both for the 219 hands data and the specimen data. Here, again, the differences are very small between the two joint models (F-test value of 0.03 and less for the radii). This makes us conclude that here, too, a single circle fit provides sufficient modelling accuracy.

4. Discussion

We used finger and wrist joint rotation data to verify the double-ovoid joint model postulated in (5). Our results show that with 99% certainty, a simple
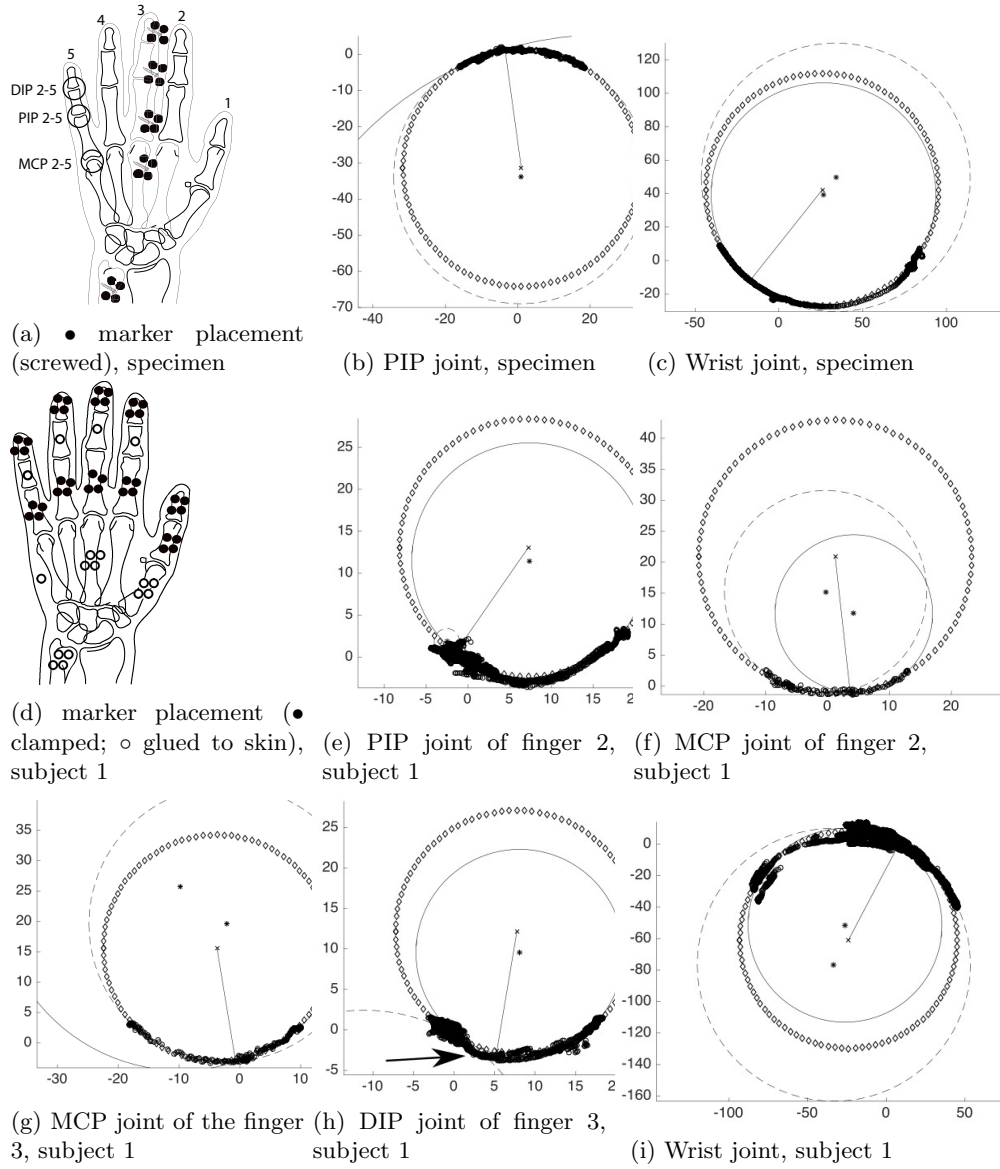
(a) • marker placement (screwed), specimen

(b) PIP joint, specimen

(c) Wrist joint, specimen

(d) marker placement (• clamped; ○ glued to skin), subject 1

(e) PIP joint of finger 2, subject 1

(f) MCP joint of finger 2, subject 1

(g) MCP joint of the finger 3, subject 1

(h) DIP joint of finger 3, subject 1

(i) Wrist joint, subject 1

Figure 1: Joints from specimen left hand (during flexion/extension of wrist, MCP, PIP and DIP) and subject 1 right hand (using data from the whole movement protocol): ○ Data, ◇ hinge joint fit, × centre hinge joint; −− double joint 1, − double joint 2, ∗ centres double joints, straight line division in the data for double hinge joint; scale in mm.

single-hinge joint model is as accurate in modelling movement of the related joints.

Accurate joint modelling is crucial for movement modelling, and influences exoskeleton and prosthesis development. Also it influences surgical procedure simulation. It impacts both medicine as robotics. Most publications (12; 13; 14; 15; 16) assume a mechanic type of joint representation for hand joints, viz. single or combined rotational joints. In contrast, (5) suggest that a double-oviod joint type is more appropriate.

While both models are approximations only, their reduced computational complexity plays an important role in numerical modelling. More complex, e.g. FEM-based, models can possibly have their merit for more accurate movement modelling, but at a very high computational cost (6). Additionally this raises the question how to obtain the necessary accurate data. While CT is appropriate from a technical point of view, it is very costly and its ionising radiation makes it unsuitable for any application that has no direct medical benefit. MRI poses an alternative, but is comparatively slow, not the best option for bone tracking, and very costly. Also, the post-processing of these data is cumbersome (14).

The method we described in this paper can easily be extended to the modelling of more complex joints with multiple axes of rotation. This can be realised by using independent component analysis (ICA) rather than PCA in the above. Apart from assuming a non-Gaussian variance—certainly a good choice for the small data sets we are using—ICA alleviates the restriction that directions of maximal variance must be perpendicular; this is, for instance, certainly true for the thumb CMC joint.

One small thing to note is the small anomalies in the circle fit for both subject1 DIP and PIP joints. This occurs as the single marker on the middle phalanges is glued to the skin and not clamped to the finger; similar results are shown in Fig. 6.2 from (9). The fact that we do not find this effect in the MCP or wrist joint, nor in the specimen recordings, fortifies our assumption of skin-induced marker movement. Results in (17) seem to confirm this assumption. We like to verify this hypothesis when evaluating the whole 219 hands data set and recording of more specimen data. Limitations of this preliminary study is the low number of one subject and one specimen recording. We verified 3D vs. 2D modelling and found no significant difference.

Conflict of interest statement

We certify that no financial or personal relationships with other people or organisations have inappropriately influenced this work.

References

[1] Y. Youm, T. Gillespie, A. Flatt, B. Sprague, Kinematic investigation of normal mcp joint, Journal of Biomechanics 11 (3) (1978) 109–118.

[2] L. Chang, N. Pollard, Robust estimation of dominant axis of rotation, Journal of Biomechanics 40 (2007) 2707–2715.

[3] J. L. Sancho-Bru, A. Pérez-González, M. Vergara, D. J. Giurintano, A 3d biomechanical model of the hand for power grip, J. Biomech. Eng. 125 (2003) 78–83.

[4] J. M. Vandeweghe, M.Rogers, M.Weissert, , Y. Matsuoka, The act hand: Design of the skeletal structure, in: Proceedings of the 2004 IEEE International Conference on Roboticsand Automation (ICRA '04), 2004, pp. 3375–3379.

[5] O. A. van Nierop, A. van der Helm, K. J. Overbeeke, T. J. Djajadiningrat, A natural human hand model, Visual Comput. 24 (2008) 31–44.

[6] K. Hollerbach, T. Axelrod, A computational model of the human hand, Tech. rep., Lawrence Livermore National Laboratory (1996).

[7] A. Goß, Development of a human finger model with the cae-software simpack, Master's thesis, University of Applied Sciences Regensburg (2012).

[8] A. Synek, G. Stillfried, Multi-body simulation of a human thumb joint by sliding surfaces, in: IEEE International Conference on Biomedical Robotics and Biomechatronics, 2012, pp. 379–384.

[9] G. Stillfried, Kinematic modelling of human hands for robotics, Ph.D. thesis, Technische Universität München (2015).

[10] G. Taubin, Estimation of planar curves, surfaces, and nonplanar space curves defined by implicit equations with applications to edge and range image segmentation, Pattern Analysis and Machine Intelligence, IEEE Transactions on 13 (11) (1991) 1115–1138.

[11] I. D. Dinov, Statistics online computational resource (socr), f distribution tables, http://www.socr.ucla.edu/applets.dir/f_table.html (July 2015).

[12] L. Chang, N. Pollard, Method for determining kinematic parameters of the in vivo thumb carpometacarpal joint, IEEE Transactions on Biomedical Engineering 55 (2008) 1897–1906.

[13] F. J. Valero-Cuevas, M. Johanson, J. D. Towles, Towards a realistic biomechanical model of the thumb: the choice of kinematic description may be more critical than the solution method or the variability/uncertainty of musculoskeletal parameters, Journal of Biomechanics 36 (7) (2003) 1019–1030. `doi:10.1016/S0021-9290(03)00061-7`.
URL `http://dx.doi.org/10.1016/S0021-9290(03)00061-7`

[14] G. Stillfried, U. Hillenbrand, M. Settels, P. van der Smagt, MRI-Based skeletal hand movement model, Springer International Publishing, 2014, pp. 49–75.

[15] A. Hollister, W. Buford, L. Myers, D. Giurintano, A. Novick, The axes of rotation of the thumb carpometacarpal joint, Journal of Orthopaedic Research 10 (1992) 454–460.

[16] D. J. Giurintano, A. M. Hollister, W. L. Buford, D. E. Thompson, L. M. Myers, A virtual five-link model of the thumb, Medical Engineering and Physics 17 (4) (1995) 297–303. `doi:10.1016/1350-4533(95)90855-6`.
URL `http://dx.doi.org/10.1016/1350-4533(95)90855-6`

[17] X. Zhang, S.-W. Lee, P. Braido, Determining finger segmental centers of rotation in flexion-extension based on surface marker measurement, Journal of Biomechanics 36 (8) (2003) 1097–1102. `doi:10.1016/S0021-9290(03)00112-X`.
URL `http://dx.doi.org/10.1016/S0021-9290(03)00112-X`